High step-up DC-DC Converter with closed loop control for Photovoltaic system with split Converter fed SRM drive

Dr Malligunta Kiran Kumar
Associate Professor
Department of Electrical & Electronics Engineering,
K L University, Vaddeswaram, Guntur, Andhra Pradesh,
India-522502
Email: kiran.malligunta@gmail.com

Kamma Mahendra
Department of Electrical & Electronics Engineering,
K L University, Vaddeswaram, Guntur, Andhra Pradesh,
India-522502

Abstract: In this paper the high step-up dc-dc converter with closed loop control is to give high voltage regulation control is reasonable for renewable energy source with split Converter fed SRM Drive. Photovoltaic system used as a renewable energy source for the dc-dc converter. This circuit comprises of active clamp circuit and step-up converter with a coupled inductor. The converter output terminal and step-up converter output terminal are associated in serially with isolated inductors with the less voltage stress on the controlled power switch and power diodes, to accomplish high output voltage gain. Moreover, to decrease circuit complexity and component number by integrated the switches in the converter and active clamp circuit with a synchronous switching technique, resulting in reduce the cost and size. The renewable energy sources based high step–up Converter with split converter-fed switched reluctance motor (SRM) drive with four-phase to understand flexible integrated charging functions in each dc and ac sources. The machine is highlighted with the eight stator slots, six rotor poles (8/6), and a central tapped winding node. The designed topology has the same characteristics as the traditional asymmetric bridge topology but good fault tolerance, in the running mode. The proposed system improves the on-board dc and ac charging and battery energy balance. When it is connecting with an ac power grid, the proposed concept has a merit of the multilevel converter; by enhanced the hysteresis control we should accomplished the charging current control. The energy flow of the both batteries is adjusted by the hysteresis control consider on their state-of-charge conditions.

Key words: DC-DC Converter, high step-up DC-DC Converter, photovoltaic System, split Converter and SRM drive.

1. INTRODUCTION

The high step-up DC-DC converters working at high voltage regulation are broadly proposed in spilt Converter fed SRM Drive. High step-up dc-dc converters [1] are taken a key role in renewable energy sources for example dc-back up energy system for UPS, photovoltaic systems, high intensity discharge lamp and automobile EV/HEV applications. The converters are used to get high dc voltage from the low dc voltage. The conventional step-up converters are get high voltage duty ratio but the problem is increasing more complexity and electromagnetic interference. In this taken method high step-up topology shown with closed loop control. Output voltage controlled with better voltage regulation for different changes in the load conditions. The dc-dc converters with coupled inductors efficiency is degraded by the losses are occurred with leakage inductors, but they can give a high voltage gain. The solution would be the utilization of transformers to get the favored voltage conversion ratio comparable in fly back or forward converter the dc-isolation is not required for industrial applications. To suppress the high voltage spike on power switch active clamp circuit and non-dissipative snubber is used. The active clamp circuit clamps the surge voltage of switches and recycles the energy stored in the leakage inductance of the transformer [5]. The leakage energy of the coupling inductor recycles the energy.

The high voltage gain DC-DC boost converters play a major role in more industry applications such as uninterrupted power supplies (UPS), distributed PV generation systems, electric traction, fuel cell energy conversion systems, automobile HID headlamps, and medical equipment. However, the PV cells output voltages are not large enough for connecting to an AC utility voltage. Series connected PV panels can provide a large DC voltage but it is difficult to avoid the shadow effect in the PV panels. High boost converters are giving a reasonable solutions for the aforementioned problem. Every PV panel is in contacted with the particular high boost converters are lift the low input voltage to high voltage level. The main advantages of high boost converters are their long conversion ratio, more efficiency and less size.

The efficiency of solar cell is consists a very low, so maximum power control of PV panel utilizing to make SPV array as an efficient, different environmental conditions and constant electrical energy source at all insolation levels. The induction motors or DC motors are used in water pumping applications. But these motors have faced from many problems like a maintainence

problem of DC motors due to the presence of brushes and commutator and the need of complex electronic inverter in case of an induction motor. In order to avoid these problems, brushless dc motors are utilized in pumping system, but these are also faced difficulties from some major problems like more converter cost, difficult control, moderate the over load capacity and irreversible demagnetizing characteristics.

However, its front-end dc–dc converter is making this topology less practical, externally equipped and comfortable for the target application. Based on the same motor, an integrated SRM charger is created to utilize standard three-phase intelligent power modules in a four-phase full-bridge converter [7]. To increase converter reliability, [8] and [9] shows a cascaded high-frequency resonant converter with a less dc-link capacitor. In [10], a maximum power tracking technology for a large state-of-charge (SoC) range is created to increase energy efficiency at both high and low-load conditions. This paper shows a split converter fed SRM with a central-tapped winding of the motor to support dc and ac grid charging, without planning of action to the charging infrastructure. This will meet adaptable charging necessities at no extra hardware investment.

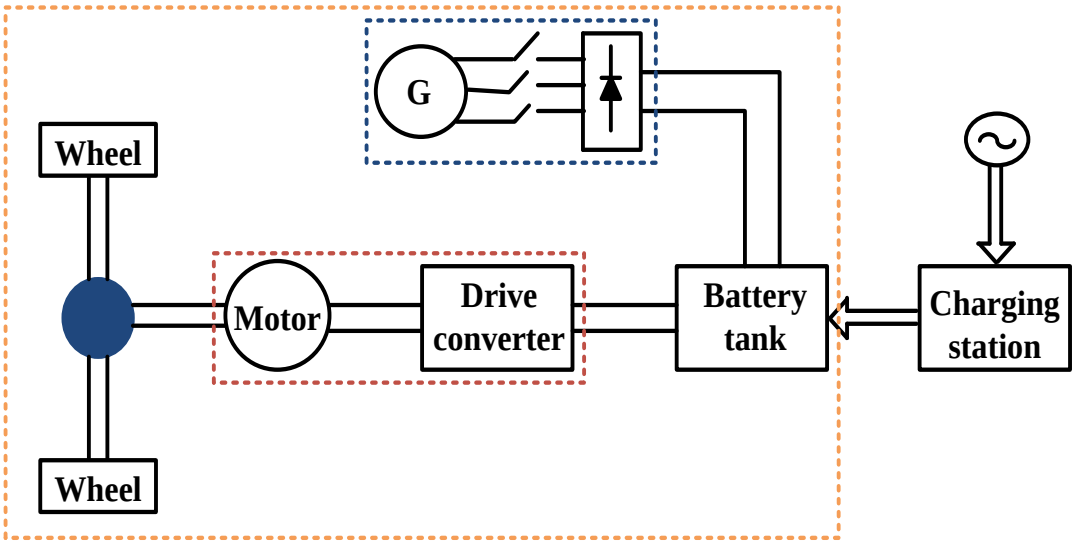

Fig.1.Basic EV/HEV drive structure.

SRMs have advantage of power full mechanical structure, less cost, more efficiency, and high speed range. However, to operate EVs/HEVs in an urban areas, a more number of charging stations should be constructed in a same way to gas stations for internal combustion engine (ICE) vehicles. A basic EV/HEV drive structure is shown in Fig. 1. Moreover, there is also a need to update the existing power grid if a more number of EVs/HEVs are connected to it. Clearly, the building costs can be similar if we were to exchange half of existing ICE cars by electrified ones within 20 years. To tackle this problem, a current trend is to develop high-power on-board chargers to full fill range limitations [11]. This is achieved by increasing the converter technologies, integrating the charger with the drive motor, or integrating the charger with the converter. The first way is shown in the example in [12], which shows a three-port dc–dc converter with power factor correction. The second way is teaching in [13], which integrates a bidirectional ac–dc charger with a dc–dc converter. In this case, the charging system can control energy flow between the high-voltage bus and the battery pack, but its circuitry is more difficult, and the available power flow modes are limited. The third way is explained in [14], which integrate the on-board charger with the drive motor, in order to use the machine winding for charging purposes. A 20-kW PM split-phase motor drive is exceptionally planned, and its traction/charging modes are controlled by switch-based relay [15], yet the motor experiences from less charging power (<3 kW) and more harmonic contents in the back electromotive force. The same tropology for a split-phase induction machine was created in [16] to give three grid-connected nodes, which can consolidate motoring and grid-charging functions.

II. SRM TOPOLOGY WITH CENTRAL-TAPPED WINDINGS

To understand grid charging without the requirement for charging stations, a split-phase structure is created for PM motors [14], [16]; however, they are suited just for ac charging and require special design of the winding structure. In this paper, a four-phase eight-slot/six-pole (8/6) SRM is taken. It can be seen that the central-tapped node is easily designed. To understand the modular shape of the motor drive, the asymmetric half-bridge converter method is developed, as seen in Fig. 2. S0~S7 are eight metal–oxide–semiconductor field effect transistors (MOSFETs), D0~D7 are eight freewheeling diodes, and Cab and Ccd are two input filter capacitors. La14, La23, Lb14, Lb23, Lc14, Lc23, Ld14, and Ld23 are the winding inductances of phases A, B, C, and D, respectively. NA, NB, NC, and ND are the central-tapped nodes of the four phases. Clearly, phases A and B share the E1 battery voltage; phases C and D share E2 battery voltage. Converter I runs phases A and B of the SRM, whereas

converter II runs phases C and D. The converter drives in two modes: one is driving and second is charging. In the driving mode, the charging plug is idle, and the converter methodology is equivalent to a traditional asymmetric half-bridge methodology. Since NA and ND didn't connect to one another, there is no current flowing between NB and NC, i.e., converters I and II are operated independently. In the charging mode, the charging plug is connected to an external power source. Converters I and II are act as charging converters.

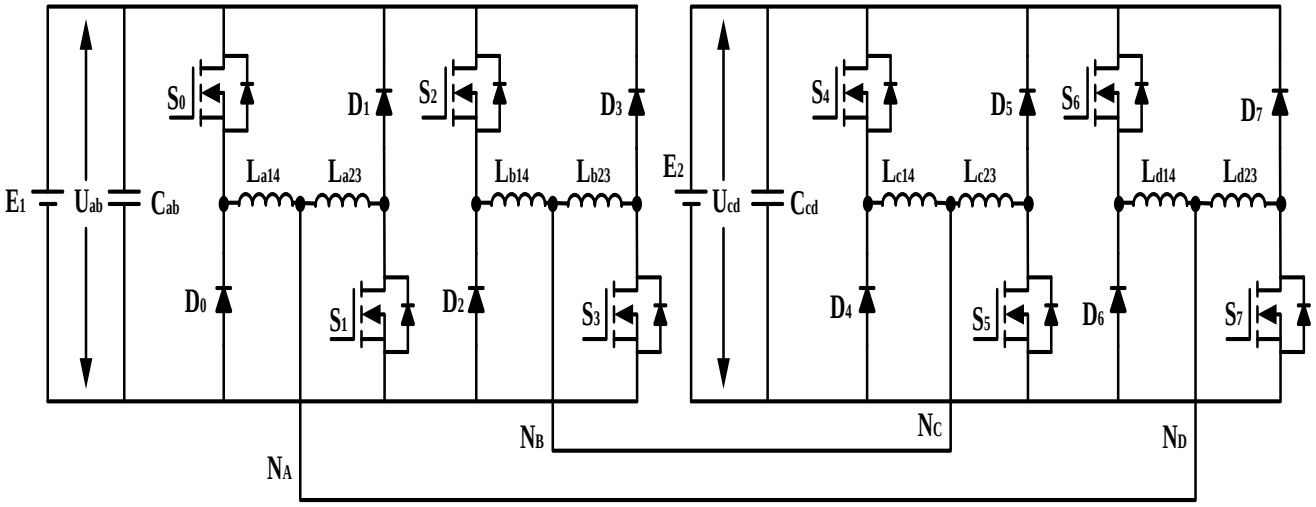

Fig. 2. Proposed topology with a central-tapped node.

A. Battery Voltage Balance Control in the Standstill Scenario

Because of a voltage distinction between the batteries and phase windings, the batteries may have different SOC levels. To level the battery voltages between phases, node NA is connected to ND in the standstill scenario, as presented in Fig. 2. When the SoC of battery E1 is more than that of battery E2, the comparing charging state circuits are shown in Fig. 3(b) and 2. In Fig. 3(a), S0 and S3 direct to charge winding inductances. In Fig. 3(b), the energy stored in winding inductors is discharged to battery E2. At the point when the SoC of battery E1 is lesser than that of battery E2, S1, S5, and S6 are switched on to charge winding inductances. By turning off devices S1 and S6, the battery E1 is charged.

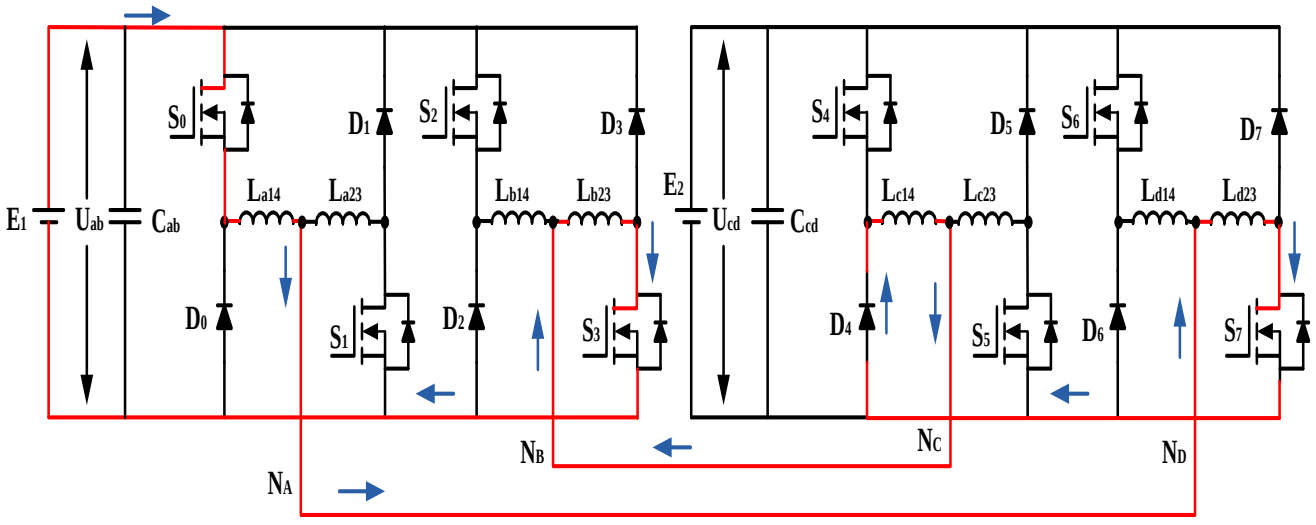

(a)

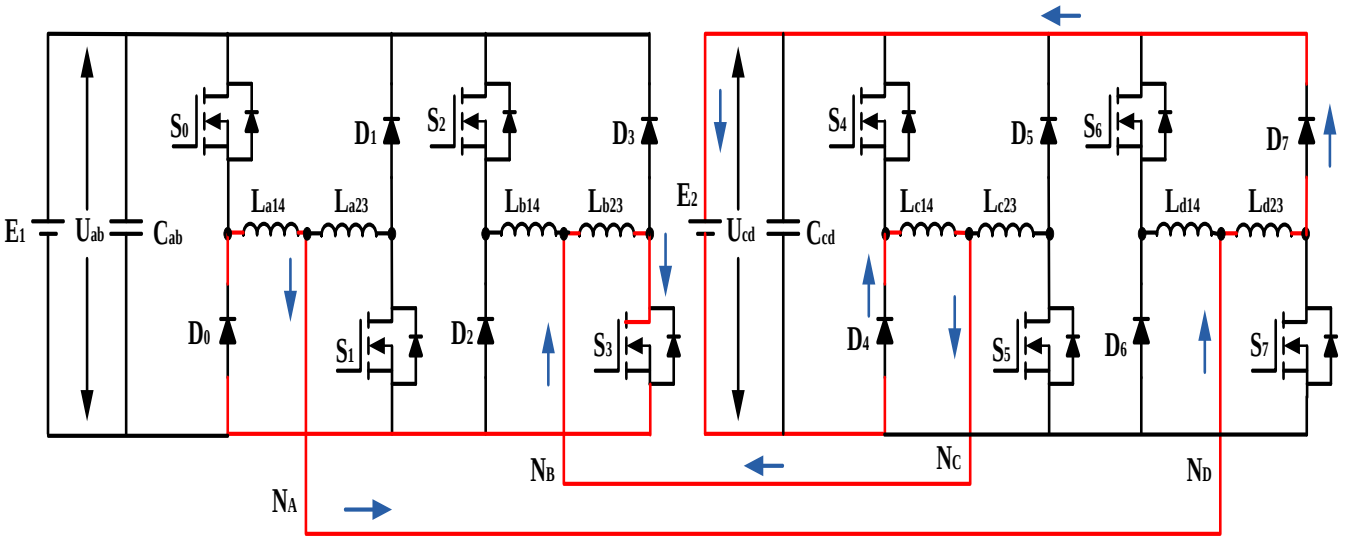

(b)

Fig. 3. Battery voltage balance at working states. (a) State of excitation of phase windings. (b) State of E2 charging.

III. CHARGING CONTROL STRATEGY

The proposed dual-split converter can support both dc and ac charging.

A. DC Power Charging

The batteries can be charged by the low-voltage dc power (e.g., from a dc micro grid), this method has a step-up voltage characteristic, and along these lines, the dc source voltage should be lesser than the sum of Uab and Ucd. Typically, the accessible dc source voltage is lesser than the twice on-board battery voltage in an EV/HEV structure, which makes the proposed strategy reasonable for the normal dc sources. There are four fundamental working states, as represented in Fig.4. In working stage 1, just S3 and S7 lead. The dc source charges the winding inductances La14, Lb23, Lc14, and Ld23; the comparing voltage equation can be expressed as

$$U_{dc}= (L_{a14}+L_{b23}+L_{c14}+L_{d23})\frac{di_S}{dt}$$

Where Udc is the outside dc source voltage, and is the output current of the dc source. In working stage 2, all MOSFETs quit conducting. The dc source and winding inductances (La14, Lb23, Lc14, and Ld23)

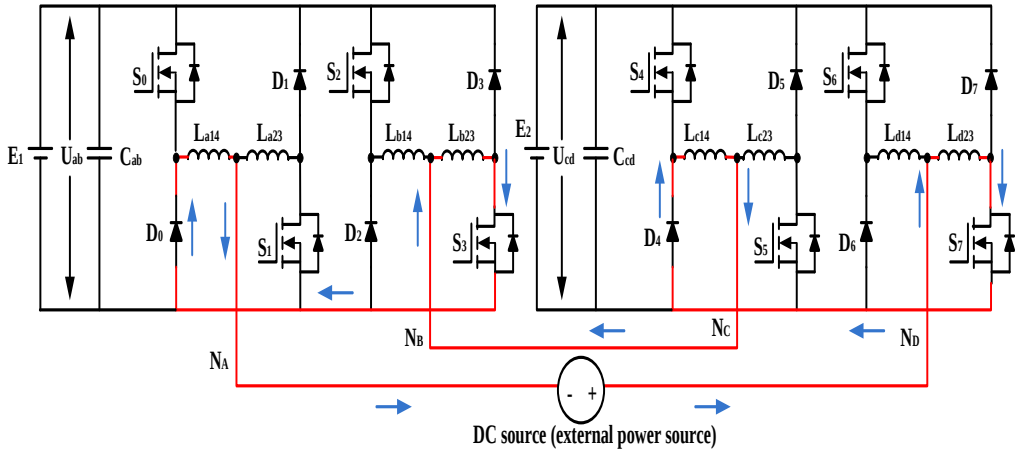

(a)

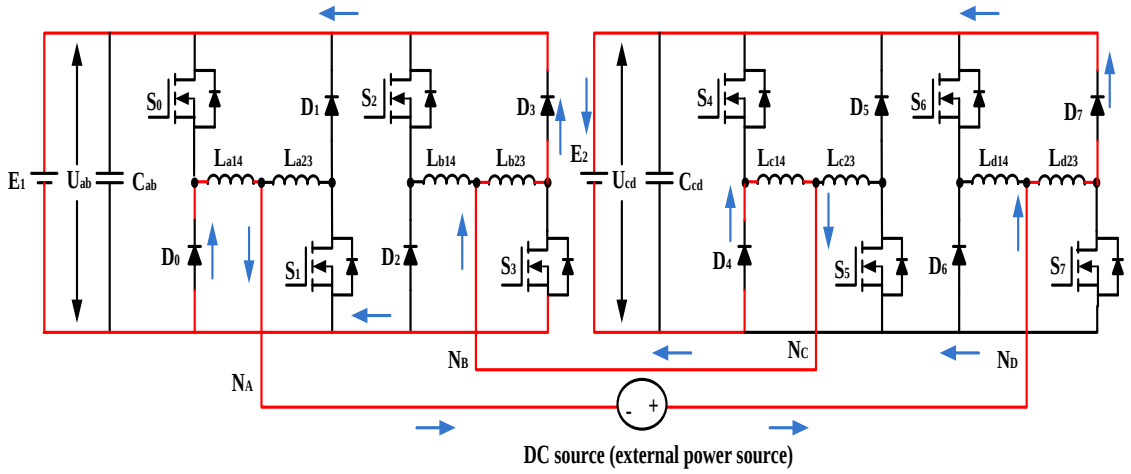

(b)

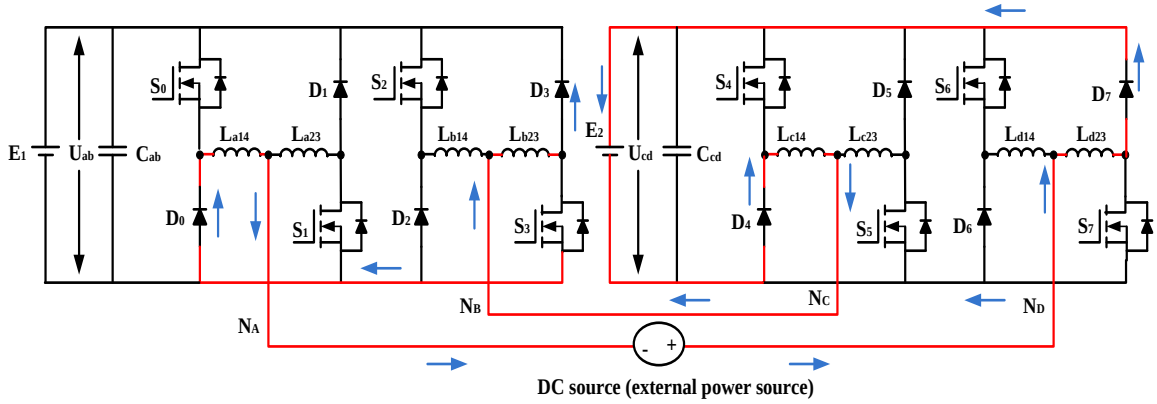

(c)

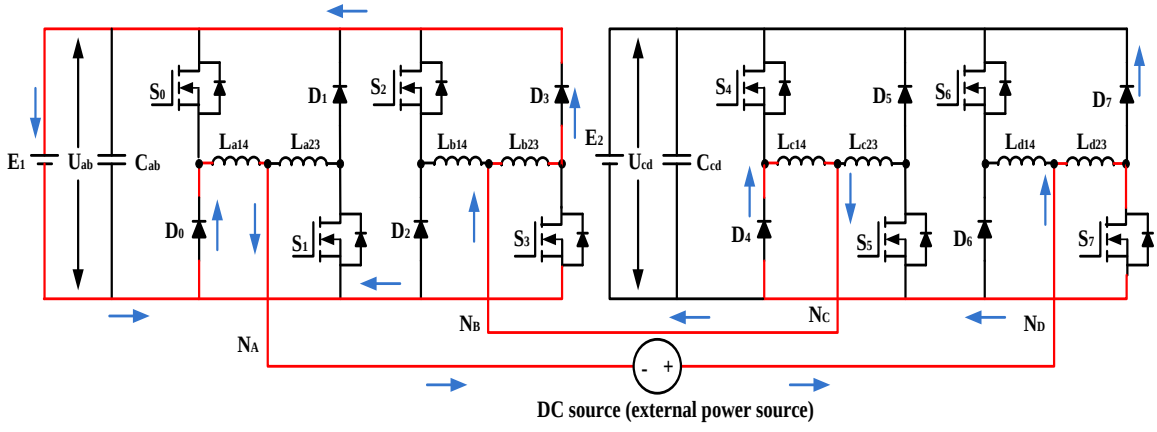

(d)

Fig.4. Working stages in low-dc-voltage charging. (a) State 1. (b) State 2. (c) State 3. (d) State 4.

Discharge the energy to the two batteries at the meantime, i.e.,

$$U_{dc}= (L_{a14}+L_{b23}+L_{c14}+L_{d23})\frac{di_s}{dt}+U_{ab}+U_{cd}$$

In working stage 3, S3 conducts. The dc source and winding inductances (La14, Lb23, Lc14, and Ld23) discharge the energy to battery E2, i.e.,

$$U_{dc}= (L_{a14}+L_{b23}+L_{c14}+L_{d23})\frac{di_s}{dt}+U_{cd}$$

In working stage 4, S7 conducts. The dc source and winding inductances (La14, Lb23, Lc14, and Ld23) discharge the energy to battery E1, i.e.,

$$U_{dc}= (L_{a14}+L_{b23}+L_{c14}+L_{d23})\frac{di_s}{dt}+U_{ab}$$

IV.HIGH STEP-UP DC-DC CONVERTER

The dc–dc converter requires large boost conversion from the panel's low voltage to the voltage level of the application. Past research on different converters for high boost applications has considered analyses of the switched-inductor and switched-capacitor types [6], [7]; transformer less switched-capacitor type, the voltage-lift type, the capacitor-diode voltage multiplier and the boost type integrated with a coupled inductor these converters by increasing turns ratio of coupled inductor gets higher voltage gain than conventional step-up converter. Some converters effectively combined step-up and fly back converters, since different converter blends are created to carry out high step-up voltage gain by utilizing the coupled-inductor strategy. The efficiency and voltage gain of the dc–dc step-up converters are compelled by either the parasitic impact of the power switches or the reverse recovery issue of the diodes.

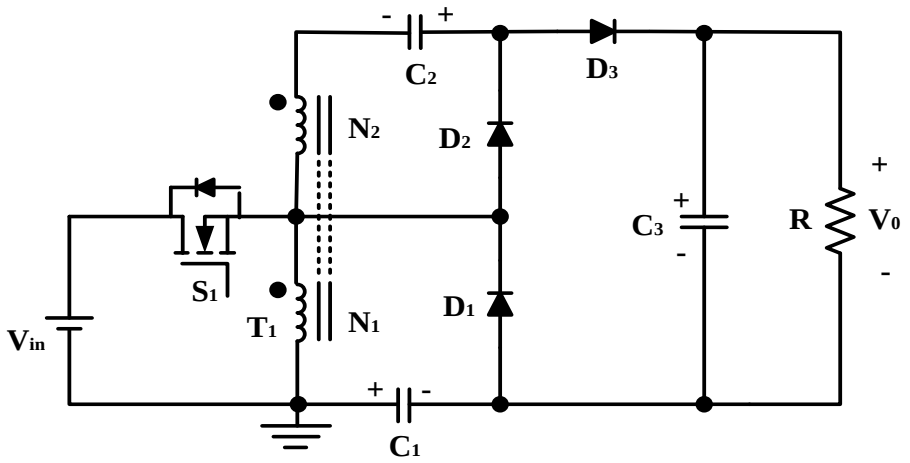

Fig.5. High step up DC-DC converter.

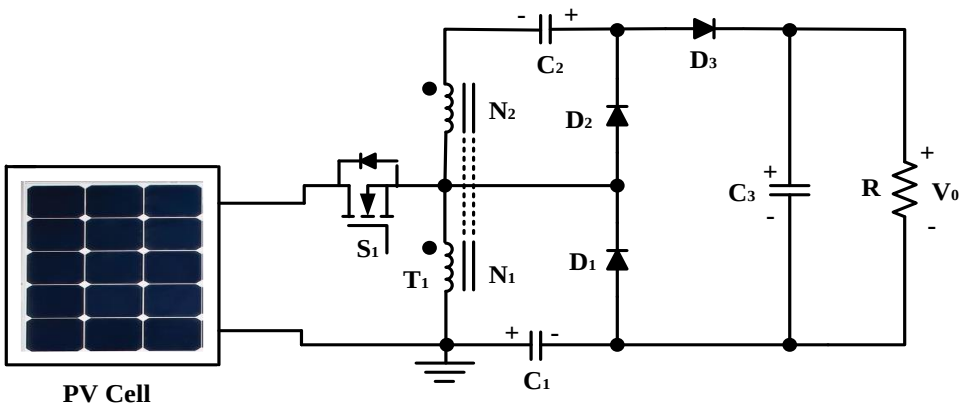

Fig.6.PV system based High step up open loop DC-DC converter.

Likewise, the equivalent series resistance (ESR) of the capacitor and the parasitic resistances of the inductor also influence overall efficiency. Utilization of active clamp method not only recycles the leakage inductor's energy but also compels the voltage stress over the active switch, however the tradeoff is higher cost and complex control circuit. By consolidating active snubber, auxiliary resonant circuit, synchronous rectifiers, or switched- capacitor-based resonant circuits and so on, these techniques did active switch into zero voltage switching (ZVS) or zero current switching (ZCS) operation and increase the converter efficiency. However, when the leakage-inductor energy from the coupled inductor can be reused, the voltage stress on the active switch is decreased, which implies the coupled inductor utilized in mix with the voltage-multiplier or voltage-lift method successfully accomplishes goal of higher voltage gain.

The converter, appeared in Fig. 7, is included of a coupled inductor T1 with the floating active switch S1. The primary winding N1 of a coupled inductor T1 is like the input inductor of the conventional step-up converter, and capacitor C1 and diode D1 get leakage inductor energy from N1. The auxiliary winding N2 of coupled inductor T1 is associated with another pair of capacitors C2 and diode D2, which are in series with N1 in order to further enlarge the lift voltage. The rectifier diode D3 interfaces to its output capacitor C3. The proposed converter has many features: 1) The connection of the two sets of inductors, capacitor, and diode gives a large step-up voltage-conversion ratio; 2) the leakage-inductor energy of the coupled inductor can be reused, hence improving the efficiency and restraining the voltage stress over the active switch; and 3) the floating active switch efficiently isolates the PV panel energy during non-operating conditions, which improves security. The working standards and steady-state analysis of the proposed converter are exhibited in the following sections.

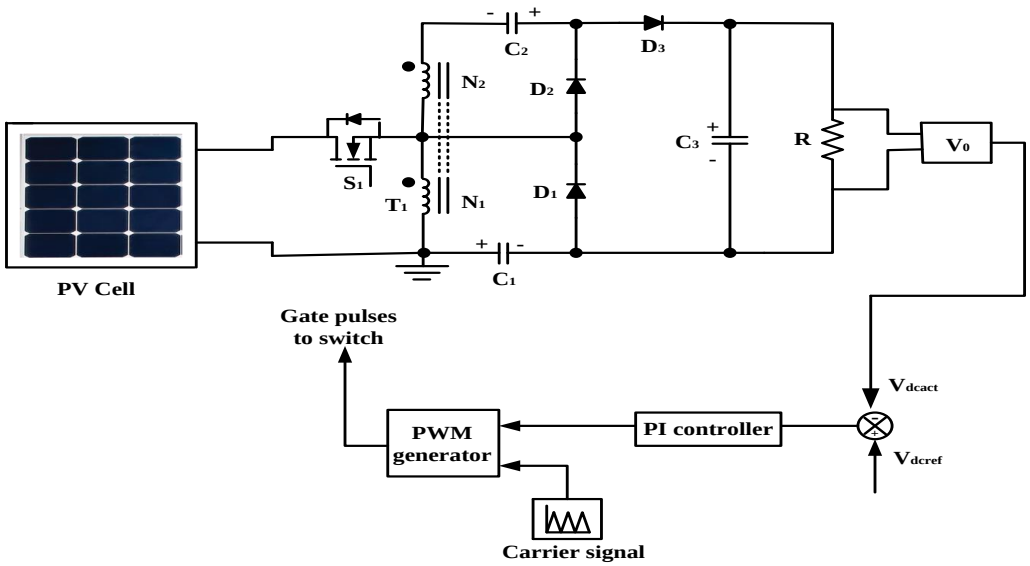

Fig.7.PV system based High step up closed loop DC-DC converter.

Two control plans are utilized in this High step up DC-DC converter. Open loop control is simpler in their layout. Because of its easy layout they are simple to construct. Since these systems don't have a feedback mechanism, they are very inaccurate in terms of result output and thus they are inconsistent as well. Because of the absence of a feedback mechanism, they are unable to remove disturbances occurring from the external sources. Closed loop control plans are more exact than open loop system because of their perplexing development. They are similarly exact and are not disturbed in the presence of nonlinearity's. Since they are made of a feedback mechanism, so get out the mistakes between input and output signals, and hence remain unaffected to the external noise sources. The closed loop PI controller is utilized as a part of the proposed converter to accomplish the desired output voltage. The PI controller consistently computes the error value as the difference between the measured process variable and a desired set point. The controller attempts to limit errors over time by conformity of a control variable. PI controllers are genuinely normal, since subordinate activity is sensitive to estimate noise. PI controller is executed here because of its several advantages. Steady state error resulting from P controller is simply overcome by the utilization of PI controller. However, the controller gives a negative effect in terms of overall stability of the system, it has a negative impact. This controller is generally employed in areas where speed of the system is not a matter. It also serves the purpose of the converter by achieving voltage regulation. Even though closed loop scheme poses the above advantages it may develop oscillatory responses of the system and it also decrease the overall gain of the system. It is less stable than open loop system but this disadvantage can be striked off since we can make the sensitivity of the system very less so as to make the system as stable as possible.

V.MATLAB/SIMULATION RESULTS

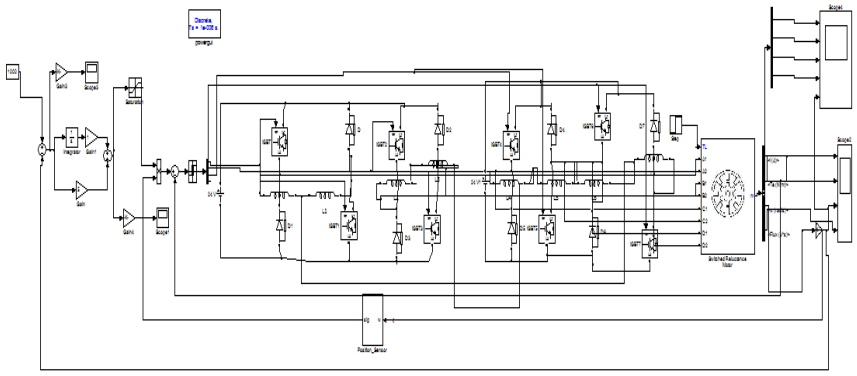

Fig.8. Matlab/Simulation model of spilt Converter fed SRM drive Converter.

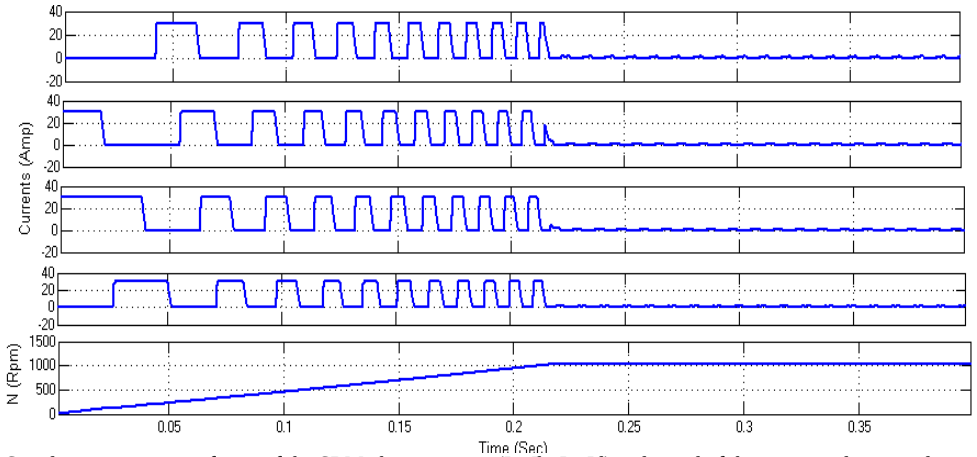

Fig.9. Simulation output waveforms of the SRM phase currents (Ia, Ib, Ic, Id) and speed of the motor under normal operation.

Fig.9. shows the output waveforms of the SRM phase currents (Ia, Ib, Ic, Id) and speed of the motor under normal operation. The output value of the phase currents approximately 35 A and speed of the motor value is 1000Rpm

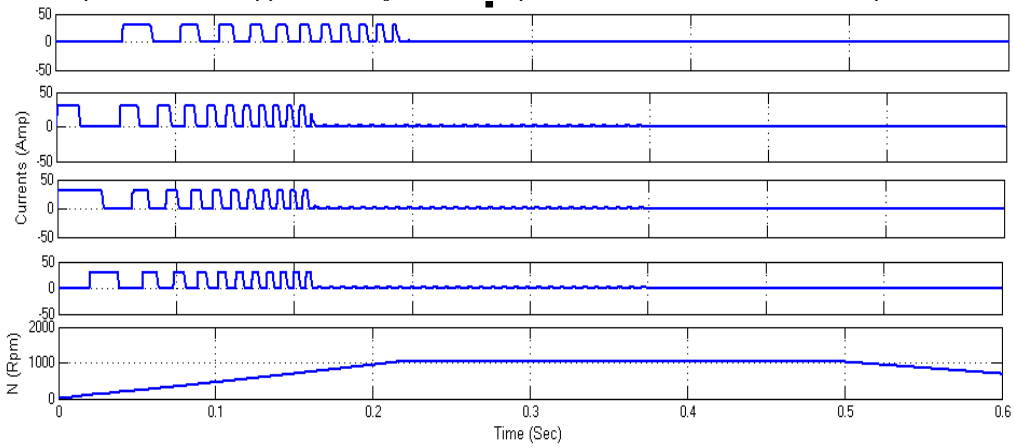

Fig.10. Simulation output waveforms of the SRM phase currents (Ia, Ib, Ic, Id) and speed of the motor braking under normal operation.

Fig.10.shows the output waveforms of the SRM phase currents (Ia, Ib, Ic, Id) and speed of the motor braking under normal operation. The output value of the phase currents approximately 40A and speed of the motor value is 1000Rpm

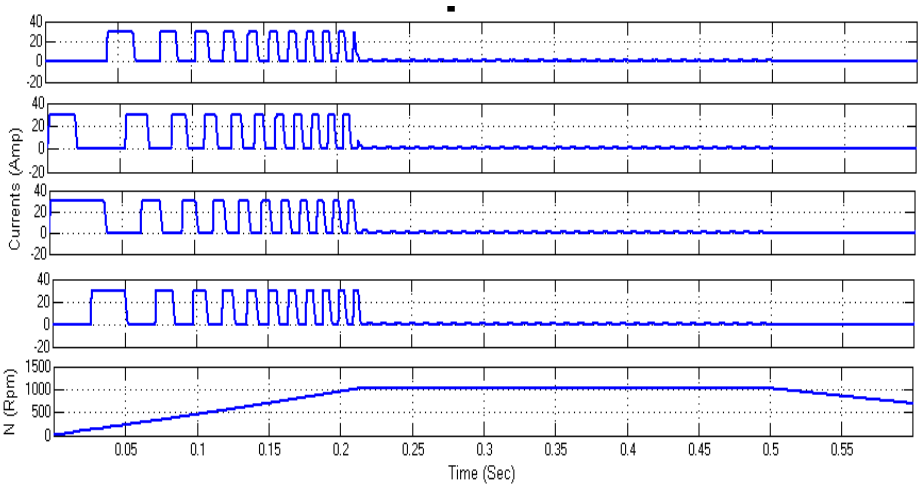

Fig.11.the output waveforms of the SRM phase currents (Ia, Ib, Ic, Id) and speed of the motor Braking under unequal SoC of the batteries operation.

Fig.11. shows the output waveforms of the SRM phase currents (Ia, Ib, Ic, Id) and speed of the motor Braking under unequal SoC of the batteries operation. The output value of the phase currents approximately 35 A and speed of the motor value is 1000Rpm

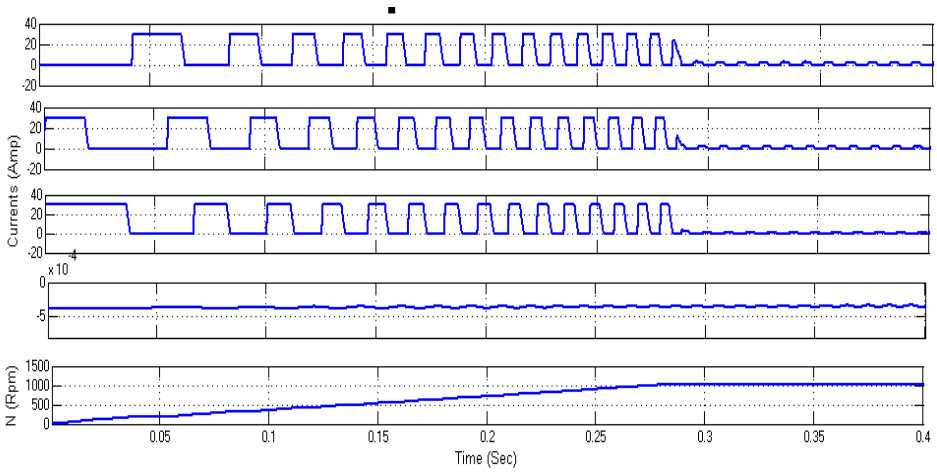

Fig.12.the output waveforms of the SRM phase currents (Ia, Ib, Ic, Id) and speed of the motor under Fault-tolerant operation.

Fig.12.shows the output waveforms of the SRM phase currents (Ia, Ib, Ic, Id) and speed of the motor under Fault-tolerant operation. The output value of the phase currents approximately 35 A and speed of the motor value is 1000Rpm.

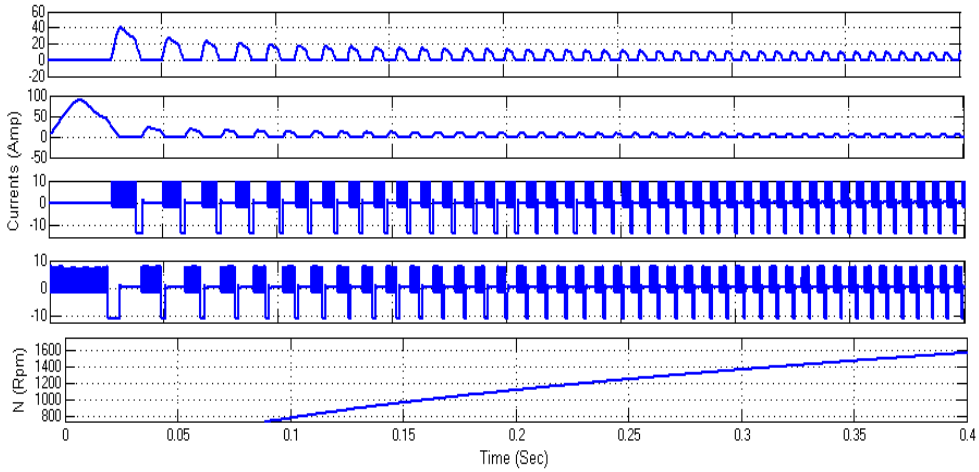

Fig.13.the output waveforms of the SRM phase currents (Ia, Ib, Ic, Id) and speed of the motor under the PWM control strategy with unequal and equal voltage sources.

Fig.13. shows the output waveforms of the SRM phase currents (Ia, Ib, Ic, Id) and speed of the motor under the PWM control strategy with unequal and equal voltage sources E1=12V and E2=-9.6V. The phase A current (40A) is straightly higher than the Phase C (10). The speed of the motor reaches to 1600 Rpm.

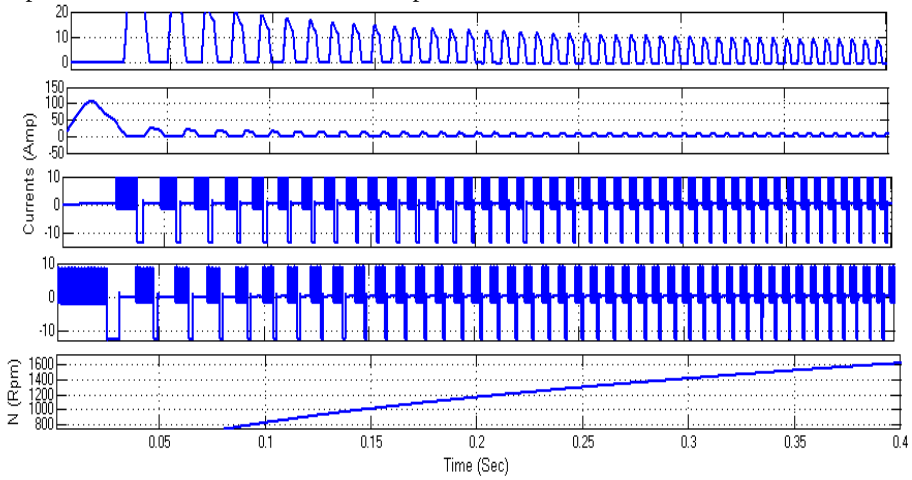

Fig.14.the output waveforms of the SRM phase currents (Ia, Ib, Ic, Id) and speed of the motor under the PWM control strategy with unequal and equal voltage sources.

Fig.14.shows the output waveforms of the SRM phase currents (Ia, Ib, Ic, Id) and speed of the motor under the PWM control strategy with unequal and equal voltage sources E1=12V and E2=-10.8V. The phase A current (15A) is straightly higher than the Phase C (10). The speed of the motor reaches to 1600 Rpm.

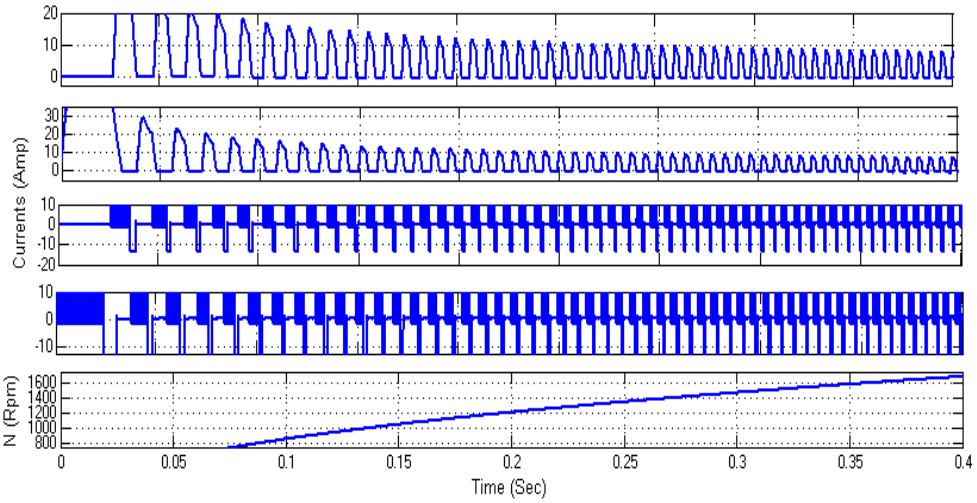

Fig .15.shows the output waveforms of the SRM phase currents (Ia, Ib, Ic, Id) and speed of the motor under the current chopping control (CCC) with unequal and equal voltage sources.

Fig.15.shows the output waveforms of the SRM phase currents (Ia, Ib, Ic, Id) and speed of the motor under the PWM control strategy with unequal and equal voltage sources E1=12V and E2=-12V. The phase A current (40A) is straightly higher than the Phase C (10). The speed of the motor reaches to 1600 Rpm.

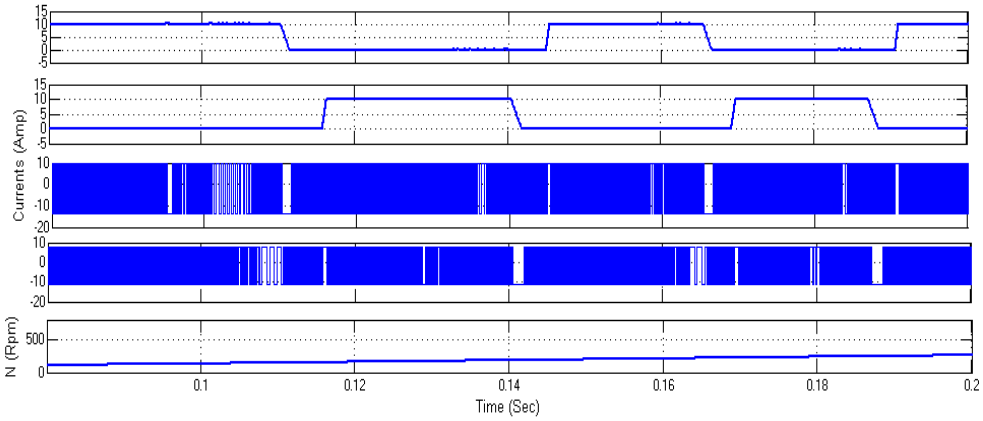

Fig.16.the output waveforms of the SRM phase currents (Ia, Ib, Ic, Id) and speed of the CCC.

Fig.16. shows the output waveforms of the SRM phase currents (Ia, Ib, Ic, Id) and speed of the motor under the current chopping control (CCC) with unequal and equal voltage sources E1=12V and E2=-9.6V

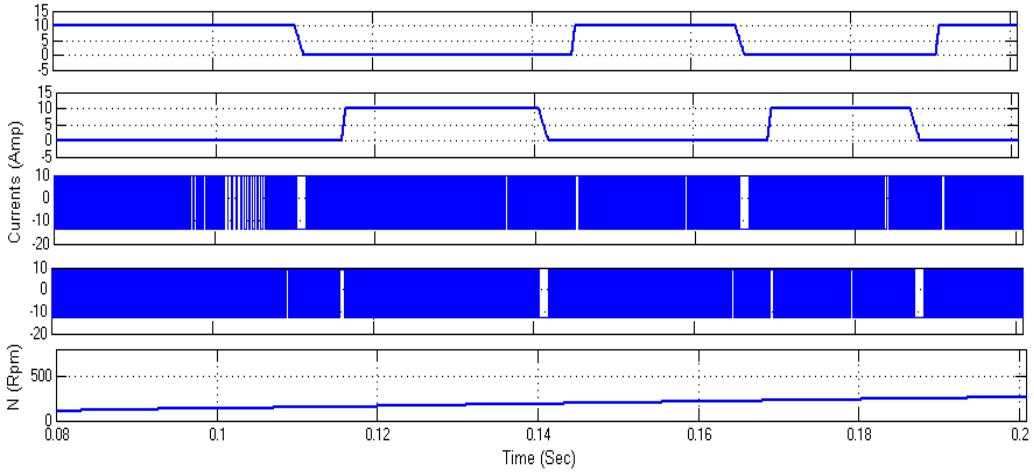

Fig.17.the output waveforms of the SRM phase currents (Ia, Ib, Ic, Id) and speed of the CCC.

Fig.17. shows the output waveforms of the SRM phase currents (Ia, Ib, Ic, Id) and speed of the motor under the current chopping control (CCC) with unequal and equal voltage sources E1=12V and E2=-10.8V.

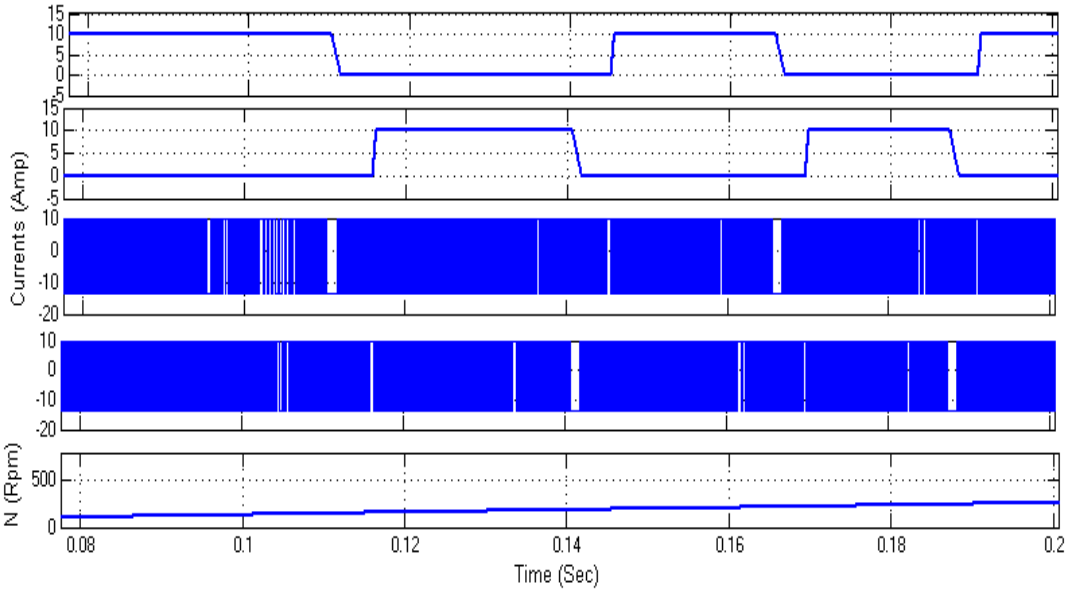

Fig.18.the output waveforms of the SRM phase currents (Ia, Ib, Ic, Id) and speed of the CCC.

Fig.18. shows the output waveforms of the SRM phase currents (Ia, Ib, Ic, Id) and speed of the motor under the current chopping control (CCC) with unequal and equal voltage sources E1=12V and E2=-10.8V.

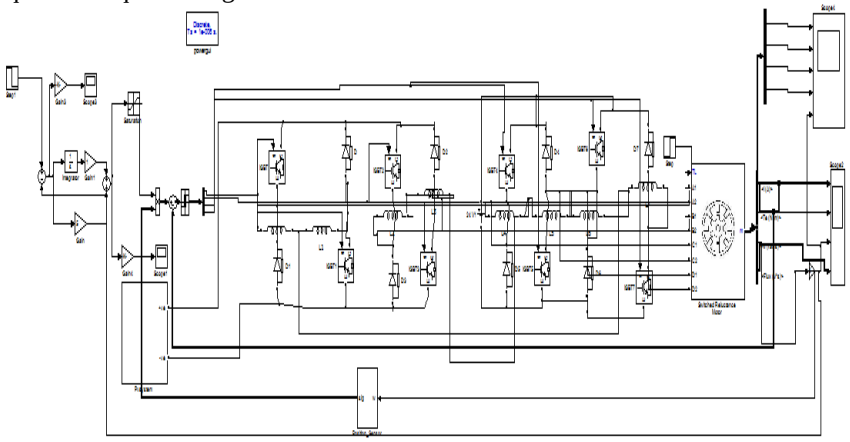

Fig.19.Matlab/Simulation model of PV system based high step DC-DC Converter fed SRM drive Converter.

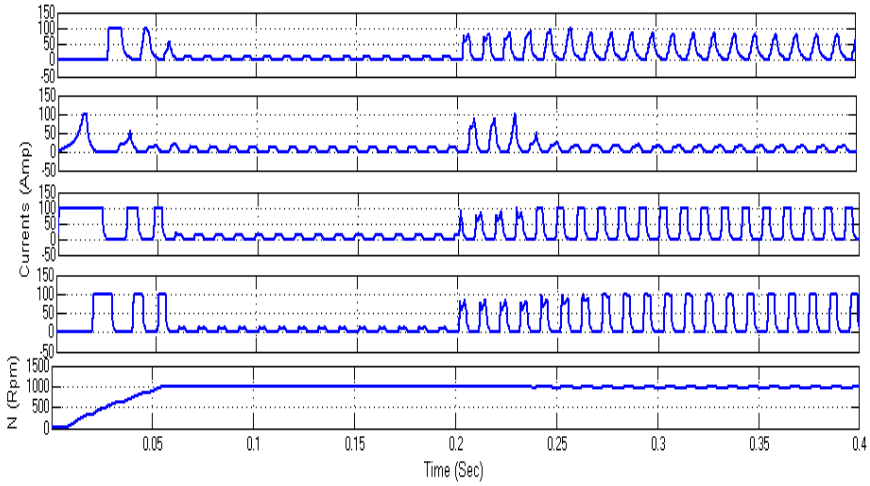

Fig.20.The output waveforms of the PV System based closed loop control of SRM phase currents (Ia, Ib, Ic, Id) and speed of the motor braking under normal operation.

Fig.20. shows the output waveforms of the SRM phase currents (Ia, Ib, Ic, Id) and speed of the motor braking under normal operation. The output value of the phase currents approximately 100A and speed of the motor value is 1000Rpm. The closed loop step-up DC-DC Converter fed SRM Drive the speed of steady state response time is 0.05sec.

VI.CONCLUSION

The high step-up dc –dc converter proposed in this paper is suitable for SRM Drive systems based on renewable energy sources which require high voltage transfer gain. The voltage stress on the main power switch is reduced therefore a switch with low on state resistance can be chosen. The proposed converter is simulated for both open loop and closed loop control and their corresponding output voltages are presented. To speed up the market acceptance of EVs/HEVs, the capital cost in charging infrastructure needs to be lower as much as possible. This paper has presented an improved asymmetric half-bridge converter-fed SRM drive to provide both driving and on-board dc charging functions so that the reliance on off-board charging stations is reduced. The main contributions of this paper are as follows it combines the split converter topology with central-tapped SRM windings to improve system reliability. The closed loop Control of High step-up DC-DC Converter fed SRM Drive. The closed loop control of SRM drive to improve the steady state response of speed.

REFERENCES

[1] T. Shimizu, K. Wada, and N. Nakamura, “Flyback-type single-phase utility interactive inverter with power pulsation decoupling on the dc input for an ac photovoltaic module system,” IEEE Trans. Power Electron., vol. 21, no. 5, pp. 1264–1272, Jan. 2006.
[2] C. Rodriguez and G. A. J. Amaratunga, “Long-lifetime power inverter for photovoltaic ac modules,” IEEE Trans. Ind. Electron., vol. 55, no. 7, pp. 2593–2601, Jul. 2008.
[3] S. B. Kjaer, J. K. Pedersen, and F. Blaabjerg, “A review of single-phase grid-connected inverters for photovoltaic modules,” IEEE Trans. Ind. Appl., vol. 41, no. 5, pp. 1292–1306, Sep./Oct. 2005.

[4] J. J. Bzura, "The ac module: An overview and update on self-contained modular PV systems," in Proc. IEEE Power Eng. Soc. Gen. Meeting, Jul. 2010, pp. 1–3.
[5] B. Jablonska, A. L. Kooijman-van Dijk, H. F. Kaan, M. van Leeuwen, G. T. M. de Boer, and H. H. C. de Moor, "PV-PRIVE project at ECN, five ´ years of experience with small-scale ac module PV systems," in Proc. 20th Eur. Photovoltaic Solar Energy Conf., Barcelona, Spain, Jun. 2005, pp. 2728–2731.
[6] T. Umeno, K. Takahashi, F. Ueno, T. Inoue, and I. Oota, "A new approach to low ripple-noise switching converters on the basis of switched- capacitor converters," in Proc. IEEE Int. Symp. Circuits Syst., Jun. 1991, pp. 1077–1080.
[7] H. C. Chang and C. M. Liaw, "An integrated driving/charging switched reluctance motor drive using three-phase power module," IEEE Trans. Ind. Electron., vol. 58, no. 5, pp. 1763–1775, May 2011.
[8] K. M. Yoo, K. D. Kim, and J. Y. Lee, "Single- and three-phase PHEV onboard battery charger using small link capacitor," IEEE Trans. Ind. Electron., vol. 60, no. 8, pp. 1763–1775, May 2013.
[9] J. Y. Lee, "An EL capacitorless EV on-board charger using harmonic modulation technique," IEEE Trans. Ind. Electron., vol. 61, no. 4, pp. 1784–1787, May 2014.
[10] H. Wang, S. Dusmez, and A. Khaligh, "Maximum efficiency point tracking technique for LLC based PEV chargers through variable DC link control," IEEE Trans. Ind. Electron., vol. 61, no. 11, pp. 6041–6049, May 2014.
[11] S. Y. R. Hui and W. W. C. Ho, "A new generation of universal contactless battery charging platform for portable consumer electronic equipment," IEEE Trans. Power Electron., vol. 20, no. 3, pp. 620–627, May 2005.
[12] C. Aguilar, F. Canales, J. Arau, J. Sebastian, and J. Uceda, "An integrated battery charger/discharger with power-factor correction," IEEE Trans. Ind. Electron., vol. 44, no. 5, pp. 597–603, Oct. 1997.
[13] Y. J. Lee, A. Khaligh, and A. Emadi, "Advanced integrated bidirectional AC/DC and DC/DC converter for plug-in hybrid electric vehicles," IEEE Trans. Veh. Technol., vol. 58, no. 8, pp. 3970–3980, Oct. 2009.
[14] S. Haghbin et al., "An integrated 20-kW motor drive and isolated battery charger for plug-in vehicles," IEEE Trans. Power Electron., vol. 28, no. 8, pp. 4013–4029, Aug. 2013.
[15] H. C. Chang and C. M. Liaw, "Development of a compact switched reluctance motor drive for EV propulsion with voltage boosting and PFC charging capabilities," IEEE Trans. Veh. Technol., vol. 58, no. 7, pp. 3198–3215, Sep. 2009.
[16] S. Haghbin, S. Lundmark, M. Alaküla, and O. Carlson, "An isolated highpower integrated charger in electrified-vehicle applications," IEEE Trans. Veh. Technol., vol. 60, no. 9, pp. 4115–4126, Nov. 2011.